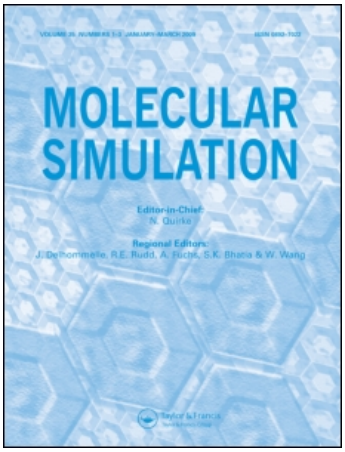

Molecular Simulation
Publication details, including instructions for authors and subscription information:
http://www.informaworld.com/smpp/title~content=t713644482

Computational analyses of virtual proteolytic fragments generated by naphthalene 1,2-dioxygenase. In search of native-like conformation and function

V. Librando[a]; A. Cambria[a]; A. Alparone[a]; D. Gullotto[a]
[a] Research Centre for Analysis, Monitoring and Minimization Methods of Environmental Risk and Department of Chemistry, University of Catania, Catania, Italy

To cite this Article Librando, V. , Cambria, A. , Alparone, A. and Gullotto, D.(2007) 'Computational analyses of virtual proteolytic fragments generated by naphthalene 1,2-dioxygenase. In search of native-like conformation and function', Molecular Simulation, 33: 3, 231 — 237
To link to this Article: DOI: 10.1080/08927020601175400
URL: http://dx.doi.org/10.1080/08927020601175400

Molecular Simulation, Vol. 33, No. 3, 15 March 2007, 231–237

Taylor & Francis
Taylor & Francis Group

Computational analyses of virtual proteolytic fragments generated by naphthalene 1,2-dioxygenase. In search of native-like conformation and function

V. LIBRANDO*, A. CAMBRIA, A. ALPARONE and D. GULLOTTO

Research Centre for Analysis, Monitoring and Minimization Methods of Environmental Risk and Department of Chemistry, University of Catania, viale A. Doria 8, Catania 95125, Italy

(Received September 2000; in final form December 2006)

Structural and energetic properties of proteolytic fragments originated from naphthalene 1,2-dioxygenase (NDO) enzyme were investigated through a computational approach. A library of fragments was generated by using an algorithm able to identify specified regions of the primary sequence and simulating cleavages on target sites. Structure of the fragments was optimised by Monte Carlo and molecular dynamics (MD) methods and the conformational and energetic properties were compared with those of the native enzyme. Protonation states of ionizable groups were predicted on the basis of effective pK_a values. Proteolytic fragments structurally similar to NDO were docked to naphthalene and interaction energies were evaluated by using MD computations. Many candidate fragments were able to maintain properties close to those which occur in the native conditions, while structures obtained by cleavages on the β-subunit of the NDO asymmetric unit were found to be rather unstable. Among the investigated structures, owing to comparable energetic and structural characteristics, 146–694 proteolytic fragment may be a promising alternative to NDO enzyme for complexation and biodegradation of naphthalenes.

Keywords: Naphthalene 1,2-dioxygenase; Proteolytic fragments; Monte Carlo; Molecular dynamics; Enzyme–substrate docking

1. Introduction

Screening of molecular combinatorial libraries takes advantage of new methods for the detection of biological active compounds, that by an increasing number of large databases are extensively employed for investigation of chemical-physics properties of molecules [1,2]. Computational tools are helpful to assist experimental studies to explore properties related to molecular interactions, especially for biologic polymers, such as DNA, proteins and enzymes [3–5]. There is great attention in development of techniques for the generation of libraries containing modified proteins with specific functional properties useful for applications in the fields of catalysis and interaction with substrates. Selection and *ex novo* design of proteins are guiding biochemical research to understand rules governing both the folding of amino acidic chains and the biological function explicated by stable native conformation enzymes [6,7]. Analysis of free energy landscapes between several folding motifs of amino acidic chains is useful to understand the laws that rule protein folding, which depending on autonomous substructures with intrinsic stability [8], arrange polypeptides towards energetically preferred conformations, before of the attainment of the native conditions. These important substructures known as closed loops, each one constituted by an average of 25–30 residues, have been recently noticed in globular proteins [9]. In both mutated and wild proteins, it is widely recognised the importance of hydrophobic residues, which play a leading role during the folding pathway, stabilizing a globular structure [10,11].

The aim of the present work is to perform a computational automated procedure for comparing structural and energetic properties of virtual molecular fragments generated by the asymmetric unit of naphthalene 1,2-dioxygenase (NDO) with the corresponding values of the native enzyme. NDO is a multi-component enzyme system expressed and purified from *Pseudomonas putida* sp. strain [12]. It is known to catalyze the oxidation of about 60 different natural and anthropic aromatic compounds of great environmental interest [13]. The first

*Corresponding author. Tel.: + 39-095-738-5201. Fax: + 39-095-580138. Email: vlibrando@dipchi.unict.it

Molecular Simulation
ISSN 0892-7022 print/ISSN 1029-0435 online © 2007 Taylor & Francis
http://www.tandf.co.uk/journals
DOI: 10.1080/08927020601175400

crystal structure of NDO was reported by Kauppi *et al.* [14]. The enzyme is an $\alpha_3\beta_3$ hexamer with each α-subunit consisting of two domain: (i) a Rieske domain which contains Rieske ferredoxin (2Fe-2S); and (ii) a catalytic domain which contains, at the active-site, one atom of mononuclear ferrous iron coordinated by His208, His213, Asp362 residues and one water molecule. The role of the β-subunit is not yet clear, but its main function appears to be structural [14]. The study of this enzyme is of great interest for the development and application of bioremediation technologies [15].

2. Methods

Libraries of enzymatic fragments were generated by using AWK programming language, specifically designed to treatment of data organized in fields and records. AWK scripts were applied to X-ray crystallographic atomic coordinates of NDO extracted from the Brookhaven Protein Data Bank (PDB access codes 1EG9 and 1O7G) [16,17]. Hydrogen atoms were added to the investigated structures at pH = 7 using the Builder module of Insight II package (Molecular Simulation Inc., San Diego, CA). A virtual pool of proteases for executing *in silico* cleavages upon NDO structure, represented by trypsin, elastase, endopeptidase, thermolysin and pepsin was chosen. Proteases were employed separately following dichotomised cutting procedures applied upon either one or both ends (C and N) of the amino acid chain. Criterions adopted to predict fragments potentially able to maintain NDO native tertiary structure, made use of hydrophobic profiles determined according to the Engelman–Steitz method [18], as well as the detection of secondary structure topologies of NDO chain (α-helixes, β-sheets) [19]. In addition, analysis of the NDO primary sequence allowed discovery of putative closed loops located within enzyme chain. Amino acid sequences located within closed loops and/or regions with high hydrophobic profile were preserved from the virtual cleavages. A more detailed description of the employed computational approach is given elsewhere [20].

The library of fragments obtained by means of this strategy was subsequently subordinated to further screenings based on Monte Carlo (MC) and molecular dynamics (MD) simulations, followed by enzyme–ligand interaction analysis. Structure of the enzymatic fragments produced by the proteolytic cleavages was optimised through Metropolis MC procedure. All the MC runs were performed using the Discover-III module of Insight-II suite of programs (Molecular Simulation Inc., San Diego, CA). Starting conditions imposed exclusion of cofactors, SO_4 molecules and ligands. The CVFF force field [21] was used throughout the MC computations. An atom based method was adopted for the treatment of the non bond interactions, using a cut-off distance of 30 Å, in order to take into account for long range interaction effects given by ionized residues, and calculate separately electrostatic, van der Waals and solvation surface area energy contributions. A steepest descendent minimization procedure was used with 500 iterations until convergence down to a gradient of 10 kcal mol^{-1} Å^{-1}, followed by a Polak Ribiere conjugate gradient minimization with 1000 iterations until a tolerance of 1.0 kcal mol^{-1} Å^{-1}. Water environment was simulated through a distant-dependent dielectric constant ($D_r = 4r_{ij}$), while water molecules enclosed in the NDO PDB structure were removed, except for one molecule placed in proximity of the active-site loop [14]. Conditions described above were chosen according to the Molecular Mechanics/Poisson–Boltzmann Surface Area (MM/PBSA) method [22,23]. Any structure obtained by MC optimizations was employed as starting point for subsequent MD simulations.

Chain fluctuation of protein fragments and enzyme–substrate docking were evaluated through MD procedures by using Discovery III and Gromos96 force field [24–26]. Naphthalene was chosen as substrate for docking. It was placed in proximity of the active-site following the published crystallographic structure of the NDO-naphthalene complex (1O7G PBD code number) [17]. MD was simulated for 500 ps, using the steepest descendent approach, followed by a conjugate gradient minimization procedure. Starting temperature of 298.0 K was controlled by a direct scalar approach, with temperature window of 10 K. Snapshot conformations were collected every 2 fs at constant volume and temperature conditions (NVT), applying a distant-dependent dielectric constant method in order to consider short range interactions. All the non bond energy contributions were calculated by using an atom based method, with a cut-off distance of 10 Å. Full flexibility was allowed throughout the investigated structures, with exception of residues in proximity of NDO-naphthalene sub pocket which were constrained to be rigid.

The main aim of this investigation was to identify proteolytic fragments characterized by relatively high stability as well as favoureable conformational and catalytic properties similar or superior to those of the parent NDO system. Fragments candidate for the simulation were selected by considering both geometric and energetic criteria. Structural validation of a fragment was determined through all-atom root-mean-squared coordinates deviations (RMSD) with respect to the corresponding observed crystallographic values, as commonly adopted in the literature. As to the energetic determinations, in the present work we evaluated van der Waals term which guarantees correct packing, electrostatic contribution which increases the specificity for the correct native fold and environmental solvation terms which ensure a correct pattern of buried hydrophobic and exposed hydrophilic residues [27]. The non-bonded free energy difference between each generated fragment and NDO native structure ($\Delta G_{nb} = \Delta G_{vdW} + + \Delta G_{Elec}$) was calculated following the linear interaction energy method [28]. Solvation area terms of non polar (ΔG_{NASA}) and polar (ΔG_{PASA}) surface energies [29–31] were computed using a water probe radius of 1.4 Å.

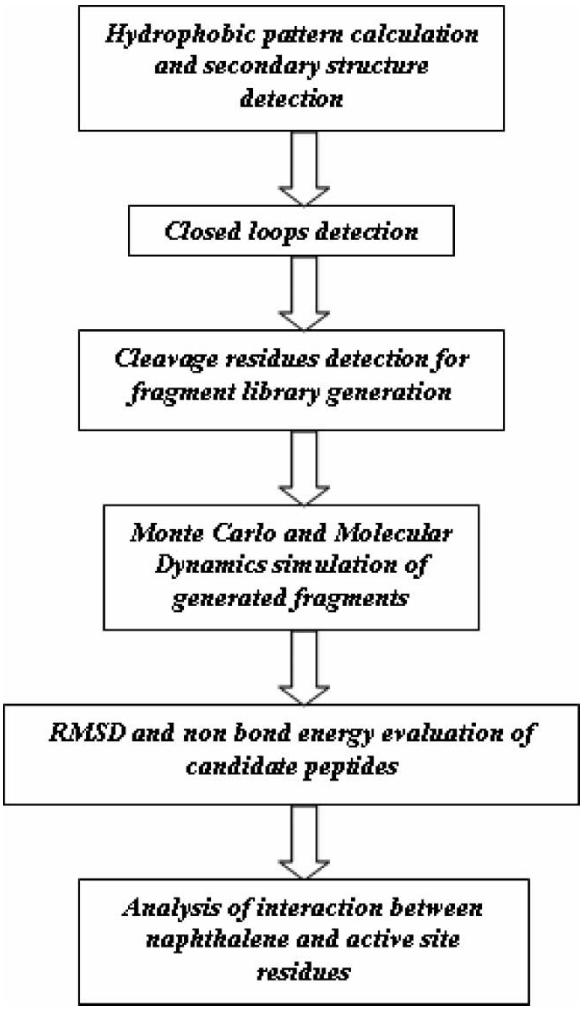

Figure 1. Schematic representation of the computational procedures applied for generation and analyses of NDO proteolytic fragments.

In figure 1 we report a schematic representation of the procedures used in the present work. The present computational approach is potentially suitable for applications on larger polycyclic aromatic hydrocarbons of significant environmental impact.

It is widely recognised that conformational stability and functionality of proteins are strongly related to pK_a values of amino acids in their specific environment [32]. Thus, we have estimated protonation states of residues in the proteolytic fragments, calculating pK_a values with the PROPKA program [33]. In a protein, the effective pK_a value of a ionizable group is determined by applying an environmental perturbation, ΔpK_a, to the intrinsic pK_{Model} value:

$$pK_a = pK_{Model} + \Delta pK_a$$

In the employed approximation, ΔpK_a value is constituted by inter-molecular hydrogen bonding, desolvation effect and charge-charge interaction contributions [33]. These terms were computed through an iterative self-consistent procedure described in details in Ref. [33]. Predicted pK_a values of residues of all the investigated fragments are available on request by the authors.

3. Results and discussion

The investigated fragments generated by proteolytic cleavages on the NDO chain are characterised by the presence of closed loops each one constituted by an average of about 30 amino acidic residues as shown in figure 2. Recently, it has been established that these structures contribute to conformational stability in the early stages of protein folding [8]. In particular, many of the detected closed loops, reveal typical fold elementary units such as α-turn-β and β-turn-β motifs, which are responsible of the compactness of the globular domains. At first, the application of the virtual cleavage generated 263 products, which after analysis of their hydropathy profile were subsequently reduced to 41. The resulting series of fragments were afterwards submitted to minimization procedures using MC and MD techniques.

In table 1 are collected the RMSD and free energy differences of the investigated fragments. The results reveal that, eight fragments (9–694, 178–694, 146–694, 148–694, 184–694, 147–694, 150–694, 189–694) show free ΔG_{TOT} values smaller than for the native enzyme. These fragments are characterised by relatively low RMSD values located in the 0.80–2.41 Å range, suggesting a substantial maintenance of the conformation of the residues of the parent NDO enzyme. As can be seen in the table, these fragments are mainly stabilised by the solvation contributions. On the whole, PASA solvation term is generally more stabilising than the NASA one. In particular one notices that, 178–694 and 184–694 fragments have the lowest NASA and PASA energy contributions, respectively, giving the lowest ΔG_{TOT} energy values along the series. It is important to note that, in these fragments the β-subunit is preserved and with the notable exception of 9–694, they reveal only two of the five detected closed-loops. Despite the loss of the 10–39, 91–115 and 142–171 closed-loops, the above fragments are, however, more stable than 102–694, 107–694, 109–694 and 117–694 ones, which have three of the five detected closed-loops. This result suggests that, 293–322 and 380–407 fragments give a fundamental contribution to the stabilisation of the modified enzymes. As expected, 9–694 and 20–694, which among the investigated fragments are structurally closer to the NDO enzyme, have the smallest RMSD values (0.80 and 0.77 Å, respectively) and contemporary the smallest ΔG_{nb} values. Specifically, fragment 9–694 shows the smallest van der Waals and electrostatic contributions along the series. Other fragments (34–694, 41–694 and 50–694) with little RMSD values (1.04–1.08 Å) have also somewhat low ΔG_{nb} values. It is worth noting that these fragments with low ΔG_{nb} values are those with show all the detected closed-loops as well as the maintenance of the β-subunit.

It is of interest to notice that for fragments with RMSD coordinate values in the 0.77–2.41 Å range, protonation states are on the whole similar to those of the parent NDO enzyme. Indeed, their root-mean-squared pK_a deviations with respect to the parent structure are predicted to be in the

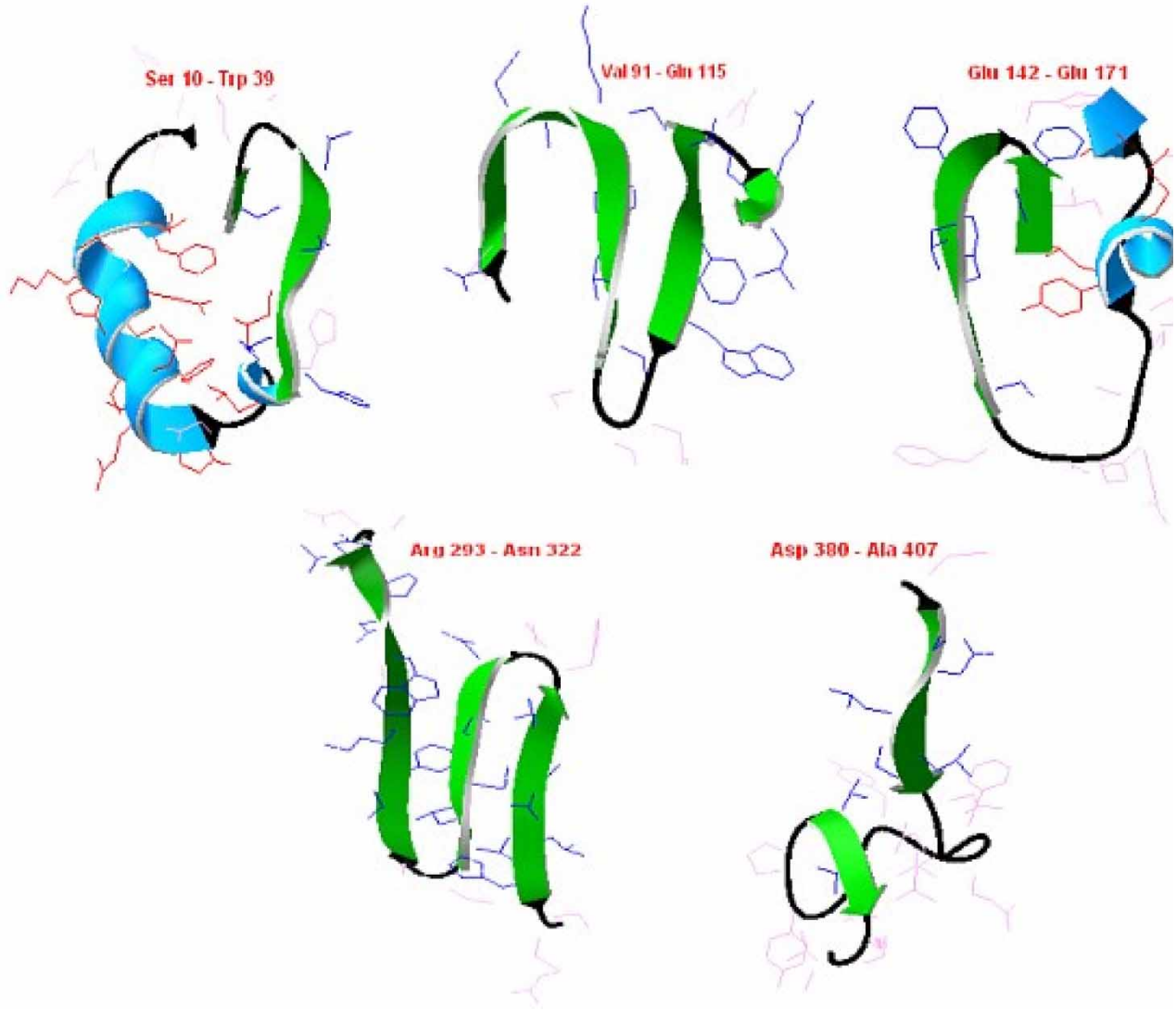

Figure 2. Solid ribbon representation of closed loops detected in the crystal structure of NDO enzyme.

0.99–1.53 range. The results show that the lowest and the largest root-mean-squared pK_a deviations are obtained for the 20–694 and 178–694 fragments, respectively, the former showing structural properties similar to those of the parent enzyme (RMSD = 0.77 Å), while the latter having the largest solvent stabilisation effect in the series. Note that for the 178–694 fragment, the largest variations of pK_a with respect to the parent enzyme are within 6–7 units and mainly involve Tyr420, His423 and Glu660 residues. It is worth to notice that both Tyr420 and His423 are buried residues for the parent enzyme, whereas they become superficial for the 178–694 fragment owing to a decrease in both the local (50%) and desolvation massive (40%) terms, which contribute to reduce and increase the effective pK_a values of Tyr420 and His423 residues, respectively. Thus, when passing from the NDO enzyme to 178–694 fragment, pK_a values for His423 and Glu660 residues increase by 6 and 7 units, respectively, owing to desolvation contributions, hydrogen bonding and charge–charge interactions with Arg37 and with His688 and Arg645, respectively. On the other hand a negative pK_a shift occurs for the Tyr420 residue (by *ca.* 6 units), principally owing to desolvation massive contributions and coulombic interactions with the Glu30 residue.

As can be seen in table 1, fragments with a cutting in the β-subunit, despite maintain all the detected closed-loops, are unstable in comparison to the native enzyme. In addition, they show large RMSD values located in the range 4.88–6.75 Å, indicating a substantial modification of the conformation with respect to the structure of the native enzyme. The results show that, this group of fragments has large positive ΔG_{TOT} values, the solvation contributions in particular the NASA term being especially large, due to the increased exposition to the solvent by non polar residues after the removal of surface amino acids by simulated cleavages. Among the investigated fragments, 65–642 one has the largest ΔG_{TOT} value owing to the largest ΔG_{NASA} term, while the fragments 9–625, 50–625 and 65–641 have the largest ΔG_{PASA}, ΔG_{Elec} and ΔG_{vdW} values, respectively.

Table 1. Free energy difference contributions (kcal/mol) and RMSD (Å) values of the investigated fragments with respect to the NDO structure.

Fragment	*RMSD*	ΔG_{vdW}	ΔG_{Elec}	ΔG_{nb}	ΔG_{PASA}	ΔG_{NASA}	ΔG_{TOT}*
20–694	0.77	5.8	60.6	66.5	−9.0	64.7	122.2
9–694	0.80	−5.2	36.0	30.8	−176.9	−15.8	−161.9
33–694	1.04	12.2	116.3	128.5	−123.7	51.1	55.9
34–694	1.04	12.9	116.1	129.0	−118.8	107.6	117.8
41–694	1.04	17.4	164.1	181.5	441.0	952.8	1575.3
117–694	1.05	29.6	346.8	376.4	−582.9	333.5	127.0
50–694	1.08	27.3	175.2	202.4	178.8	717.8	1099.0
110–694	1.09	31.3	330.4	361.8	−270.1	382.8	474.5
178–694	1.09	1.9	427.9	429.8	−1838.2	−1296.9	−2705.3
146–694	1.11	14.2	396.8	411.0	−1406.2	−1030.7	−2025.9
148–694	1.11	11.1	392.1	403.3	−1135.8	−616.4	−1348.9
102–694	1.12	35.4	325.5	360.9	−201.8	544.6	703.7
107–694	1.12	34.3	334.3	368.6	−238.5	410.7	540.8
116–694	1.12	30.3	350.9	381.1	−565.9	308.0	123.2
184–694	1.14	3.2	436.1	439.3	−1867.8	−1262.8	−2691.3
108–694	1.15	31.8	334.9	366.7	96.8	1212.8	1676.3
147–694	1.15	12.1	395.6	407.8	−1222.3	−468.4	−1282.9
109–694	1.17	31.9	332.8	364.6	−218.4	429.8	576.0
150–694	1.27	4.4	414.4	418.8	−1482.6	−1112.1	−2175.9
189–694	2.41	12.3	446.2	458.5	−1766.5	−1049.9	−2357.9
9–627	4.88	20.3	442.1	462.4	−325.3	23.0	160.1
1–625	4.93	22.2	410.4	432.7	−151.5	112.5	393.7
1–627	4.96	20.8	412.9	433.8	125.1	1070.9	1629.8
9–625	4.97	21.7	439.6	461.3	1123.9	−884.0	701.2
1–621	5.12	21.8	419.6	441.3	125.7	978.3	1545.3
1–642	5.27	15.0	309.1	324.0	370.0	1018.2	1712.2
50–625	5.29	47.4	518.1	565.5	29.1	826.8	1421.4
9–641	5.31	18.8	376.4	395.2	78.1	328.9	802.2
9–642	5.31	18.7	377.4	396.2	482.2	1143.3	2021.6
20–642	5.36	28.3	411.6	439.9	577.7	1368.2	2385.8
33–641	5.63	30.4	422.9	453.3	50.5	1032.2	1536.0
34–641	5.70	31.7	421.9	453.6	163.0	1100.8	1717.4
41–641	5.71	39.6	481.1	520.7	433.7	1284.8	2239.2
41–642	5.71	34.5	464.1	498.6	323.9	1560.5	2383.0
50–641	5.79	45.9	483.6	529.6	433.7	1062.5	2025.8
65–641	5.88	53.5	496.2	549.7	716.0	1310.5	2576.2
20–641	6.31	28.3	410.1	438.4	321.4	1349.5	2109.3
34–642	6.56	31.6	422.9	454.6	168.2	1141.2	1763.9
33–642	6.58	30.3	423.9	454.3	−14.4	682.9	1122.8
65–642	6.75	53.4	497.6	551.0	937.9	2309.9	3798.8

* $\Delta G_{\mathrm{TOT}} = \Delta G_{\mathrm{nb}} + \Delta G_{\mathrm{NASA}} + \Delta G_{\mathrm{NASA}}$.

These results point out the fundamental function of the β-subunit in preserving a favourable conformation, guaranteeing stability in the structure of the fragments, in agreement with experimental findings, which indicate the crucial role of β-subunit in the maintenance of the native tertiary structure [12].

Fragments with RMSD values smaller than 2.5 Å, were selected to perform docking calculations with naphthalene. Binding energies of the amino acid residues of the active-site of the NDO were calculated by using GROMOS 96 force field [24–26]. The results are listed in table 2. According to information of X-ray measurements [14,16,17,21], the active-site is composed by the following residues: Asn201, Phe202, Val260, Trp 316, Thr351, Phe353, Trp358, Asp362, Met366. Note that, φ and ψ torsion angle values of active-site residues are located within the recommended ranges of the Ramachandran plot (data not shown), suggesting the maintenance of native-like conformation. In addition the root-main squared fluctuation (RMSF) range of the active reaction loop appears to be consistent with the X-ray structure (see table 3). As can be seen in table 2, interaction energy between naphthalene and Asn201 is stabilizing for all the fragments, nevertheless with large fluctuation of values. The stabilizing effect of the Asn201 residue is mainly due to the presence of a hydrogen bond between the NH_2 group of the fragment and a π ring of the substrate. This effect is particularly noticeable for 20–694, 117–694, 178–694, 146,–694 and 108–694 fragments, which show the NH_2 group significantly close to a ring of naphthalene. On the other hand, in all the cases, Phe352 and Trp316 residues give destabilizing contributions to the binding energy of the fragment-substrate system. Except for 150–694 and 102–694 fragments, Thr351 gives a stabilizing contribution to binding energy with naphthalene. As concerns remaining residues, their interaction energy can be either stabilizing or destabilizing. It is interesting to note that, the largest binding energy fluctuation among the fragments is found for Asp362 residue. This residue is strongly stabilizing for the NDO enzyme, with a binding energy comparable to that of Asn201, while for the other fragments its contribution is less important, and in some cases even destabilizing. Note also that, among the investigated fragments it shows a conspicuous RMSF

Table 2. Binding energy for residue (kcal/mol) of the investigated fragments with naphthalene.

*Fragment**	*Asn201*	*Phe202*	*Val260*	*Trp316*	*Thr351*	*Phe352*	*Trp358*	*Asp362*	*Met366*
1OG7	−26.0	1.0	−1.4	14.8	−7.2	18.0	−5.1	−23.4	7.1
20–694	−30.4	−1.8	−1.2	12.8	−8.4	19.0	12.6	−1.7	4.2
9–694	−22.9	3.0	1.9	7.6	−0.8	17.5	11.5	2.7	−0.4
33–694	−21.6	−1.0	1.4	3.5	−5.2	12.8	−3.1	11.1	4.5
34–694	−22.2	5.0	−4.1	22.6	−8.8	10.6	−0.4	4.0	3.9
41–694	−12.4	8.3	−1.1	11.8	−7.7	16.1	0.1	17.4	−3.9
117–694	−36.0	3.9	1.7	27.1	−8.8	10.0	−3.4	−1.9	3.9
50–694	−23.3	−2.7	0.0	12.4	−5.7	5.9	−3.0	17.5	−0.3
110–694	−25.9	2.3	3.7	15.5	−7.7	11.5	8.2	15.4	−0.5
178–694	−41.0	−4.9	2.5	17.1	−3.4	10.3	11.1	−1.0	5.4
146–694	−29.5	−0.2	−2.5	8.7	−3.9	15.4	−3.1	−4.3	−2.0
148–694	−24.4	0.2	7.2	12.4	−6.0	11.5	8.1	3.5	−0.8
102–694	−16.7	8.5	5.8	7.8	2.2	14.0	12.8	−0.2	0.5
107–694	−23.5	6.1	−1.2	10.5	−6.0	14.7	3.1	4.5	1.8
116–694	−15.7	−1.5	−2.2	4.1	−8.1	15.1	3.2	1.8	7.4
184–694	−16.0	−2.4	−1.3	17.0	−6.7	11.7	−1.6	−0.2	3.3
108–694	−38.4	14.8	7.6	12.1	−3.9	19.5	0.5	2.0	10.3
147–694	−18.3	−5.7	−0.3	7.9	−1.2	15.2	−2.6	−7.9	5.4
109–694	−25.1	1.8	1.6	10.0	−5.7	12.7	−3.2	0.4	2.3
150–694	−21.4	2.3	−4.3	3.8	0.2	12.5	1.3	3.3	−2.8
189–694	−26.0	0.5	0.2	15.5	−12.0	12.6	6.9	19.4	−1.9

* Fragments in the 0.77–2.41 Å RMSD range.

variation (1.09 Å). As can be seen in table 3, the largest RMSF fluctuation is predicted for Met366 residue. On the other hand, the minor binding energy fluctuation occurs for Val260, which is consistent with the lowest RMSF variation among the investigated fragments (0.54 Å). It is worth noting that, for the 146–694 fragment, which holds about 80% of the residues of NDO (RMSD = 1.11 Å, table 1), the binding energy contributions from the residues of the active site is on the whole comparable to that of the native NDO enzyme. Specifically, for this modified enzyme, seven residues (Asn201, Phe202, Val260, Thr351, Trp358, Asp362, Met366) on nine give stabilizing binding energy contributions. In particular, in six (Asn201, Phe202, Val260, Trp316, Phe352, Met366) on nine residues of 146–496 fragment, the stabilizing effect is greater than that predicted for the NDO enzyme. Thus the 146–496 proteolytic fragment may be considered a promising alternative to NDO enzyme for the complexation and biodegradation of naphthalenes. For this fragment, the RMS pK_a deviation is predicted to be 1.45, the largest variations being found for Cys309, Asp362, Tyr420 and Glu518 residues. With specific reference to the Asp362 residue, which is part of the catalytic active site, in going from the parent enzyme to the 146–694 fragment one notices an increase of the pK_a value from *ca.* 0 to 6.6, contributing to reduce the hydrophobic character and capacity of the residue to bind the ligand. The above pK_a increase mainly originates from both side-chain and

Table 3. Root mean squared fluctuation (Å) of the NDO-naphthalene active site residues*.

Fragment	*Asn 201*	*Phe 202*	*Val 260*	*Trp 316*	*Thr 351*	*Phe 352*	*Trp 358*	*Asp 362*	*Met 366*
20–694	1.59	1.11	0.83	0.59	0.57	0.51	0.33	0.52	1.71
9–694	0.64	0.47	1.05	0.71	0.36	0.83	0.4	1.35	2.26
33–694	0.67	0.34	0.92	0.36	0.48	0.54	0.55	1.41	1.29
34–694	1.28	0.49	0.68	0.79	0.54	1.4	0.25	0.89	0.88
41–694	0.61	0.49	0.79	0.92	0.81	1	0.63	0.78	1.19
117–694	0.79	0.62	0.68	1.06	0.48	1.02	0.45	0.65	2.05
50–694	1.46	0.94	0.76	0.66	0.34	0.69	0.71	1.47	1.31
110–694	1.65	0.87	0.65	0.57	0.63	0.74	0.7	0.97	1.74
178–694	0.92	0.67	0.76	0.75	0.31	0.41	0.42	0.69	1.04
146–694	0.93	0.75	0.97	0.48	0.4	0.94	0.44	0.79	1.23
148–694	1.22	0.68	0.81	0.43	0.4	0.38	0.78	1.31	1.76
102–694	1.54	0.71	0.92	0.73	0.35	0.65	0.66	1.18	1.61
107–694	1.09	0.91	0.95	0.93	0.65	0.64	1.09	0.88	0.93
116–694	0.84	0.61	0.61	0.41	0.58	0.93	1.13	0.49	2.47
184–694	0.93	0.48	0.7	0.52	0.72	0.86	0.5	0.67	1.11
108–694	1.33	0.92	0.89	0.72	0.46	1.01	0.4	0.69	2.52
147–694	1.03	0.46	0.82	1.16	0.58	1.03	0.76	0.85	1.81
109–694	0.69	0.55	1.02	0.78	0.35	0.74	0.79	1.08	1.21
150–694	0.75	1.15	0.97	0.55	0.43	0.5	0.41	0.59	1.32
189–694	0.63	0.4	0.85	0.61	0.95	0.76	1.24	1.56	0.85
1O7G	1.24	0.51	0.51	0.5	0.44	0.46	0.42	0.47	0.76

* Amino acid displacements of each fragment are calculated with respect to the NDO-naphthalene complex.

backbone hydrogen bonding interactions with Thr308 and Ser294, respectively, as well as from the coulombic term with the Glu333 residue. In addition, as previously found for the 178–694 fragment, we notice that in passing from the parent enzyme to the 146–694 fragment, Tyr420 change from buried to surface residue, owing to a decrease of both the local (from 0 to 2) and desolvation massive effects (by *ca.* 40%), in some consistency with their somewhat different solvent stabilization contributions.

Acknowledgements

This work was supported by MIUR, Rome and makes use of results produced by the PI2S2 Project managed by the Consorzio COMETA, a project co-funded by the Italian Ministry of University and Research (MIUR) within the Piano Operativo Nazionale "Ricerca Scientifica, Sviluppo Tecnologico, Alta Formazione" (PON 2000–2006). More information is available at http://www.pi2s2.it and http://www.consorzio-cometa.it.

References

[1] O.H. Villar, T.R. Koehler. Comments on the design of chemical libraries for screening. *Mol. Div.*, **5**, 13 (2000).
[2] A.D. Bosley, M. Ostermeier. Mathematical expressions useful in the construction, description and evaluation of protein libraries. *Biomol. Eng.*, **22**, 57 (2005).
[3] B.I. Dahiyat, S.L. Mayo. *De Novo* protein design: fully automated sequence selection. *Science*, **278**, 82 (1997).
[4] Y. Tang, L. Nilsson. Interaction of human SRY protein with DNA: a molecular dynamics study. *Proteins Struct. Funct. Genet.*, **31**, 417 (1998).
[5] K.W. Lee, J.M. Briggs. Molecular modeling study of the editing active site of *Escherichia coli* Leucyl-tRNA Synthetase: two amino acid binding sites in the editing domain. *Proteins Struct. Funct. Bioinf.*, **54**, 693 (2004).
[6] H.H. Tsai, C.J. Tsai, B. Ma, R. Nussinov. *In silico* protein design by combinatorial assembly of protein building blocks. *Protein Sci.*, **13**, 2753 (2004).
[7] M. Jacobson, A. Sali. Comparative protein structure modeling and its applications to drug discovery. *Ann. Rep. Med. Chem.*, **39**, 259 (2004).
[8] I.N. Berezovsky, E.N. Trifonov. Protein structure and folding: a new start. *J. Biomol. Struct. Dyn.*, **19**, 397 (2001).
[9] I.N. Berezovsky, A.Y. Grosberg, E.N. Trifonov. Closed loops of nearly standard size: common basic element of protein structure. *FEBS Lett.*, **466**, 283 (2000).
[10] S.M. Malakauskas, S.L. Mayo. Design, structure and stability of a hyperthermophilic protein variant. *Nat. Struct. Biol.*, **5**, 470 (1998).
[11] B. Kuhlman, D. Baker. Exploring folding free energy landscapes using computational protein design. *Curr. Opin. Struct. Biol.*, **14**, 89 (2004).
[12] B.D. Ensley, D.T. Gibson. Naphthalene dioxygenase: purification and properties of a terminal oxygenase component. *J. Bacteriol.*, **155**, 505 (1983).
[13] S.M. Resnick, K. Lee, D.T. Gibson. Diverse reactions catalyzed by naphthalene dioxygenase from Pseudomonas sp. strain NCIB 9816. *J. Ind. Microbiol.*, **17**, 438 (1996).
[14] B. Kauppi, K. Lee, E. Carredano, R.E. Parales, D.T. Gibson, H. Eklund, S. Ramaswamy. Structure of an aromatic-ring-hydroxylating dioxygenase-naphthalene 1,2-dioxygenase. *Structure*, **6**, 571 (1998).
[15] D.T. Gibson, R.E. Parales. Aromatic hydrocarbon dioxygenases in environmental biotechnology. *Curr. Opin. Biotechnol.*, **11**, 236 (2000).
[16] E. Carredano, A. Karlsson, B. Kauppi, D. Choudhury, R.E. Parales, J.V. Parales, K. Lee, D.T. Gibson, H. Eklund, S. Ramaswamy. Substrate binding site of naphthalene 1,2-dioxygenase: functional implications of indole binding. *J. Mol. Biol.*, **296**, 701 (2000).
[17] A. Karlsson, J.V. Parales, R.E. Parales, D.T. Gibson, H. Eklund, S. Ramaswamy. Crystal structure of naphthalene dioxygenase: side-on binding of dioxygen to Iron. *Science*, **299**, 1039 (2003).
[18] D.M. Engelmann, T.A. Steitz, A. Goldmann. Identifying nonpolar transbilayer helices in amino acid sequences of membrane proteins. *Annu. Rev. Biophys. Chem.*, **115**, 321 (1986).
[19] B. Rost. Review: protein secondary structure prediction continues to rise. *J. Struct. Biol.*, **134**, 204 (2001).
[20] V. Librando, D. Gullotto, Z. Minniti. Automated molecular library generation of proteic fragments by virtual proteolysis for molecular modelling studies. *In Silico Biol.*, **6**, 42 (2006).
[21] P.L. Dauber-Osguthorpe, V.A. Roberts, D.J. Osguthorpe, J. Wolff, M. Genest, A.T. Hagler. Structure and energetics of ligand-binding to proteins: *Escherichia coli* dihydrofolate reductase trimethoprim, a drug receptor system. *Proteins Struct. Funct. Genet.*, **4**, 31 (1988).
[22] F. Fogolari, A. Brigo, H. Molinari. Protocol for MM/PBSA molecular dynamics simulations of proteins. *Biophys. J.*, **85**, 159 (2003).
[23] M. Smith, M. Lamb, J. Rives, W. Jorgensen, C. Michejda, S. Ruby, R. Smith. Monte Carlo calculations on HIV-1 reverse transcriptase complexed with the non nucleoside inhibitor 8-Cl TIBO: contribution of the L100I and Y181C variants to protein stability and biological activity. *Protein Eng.*, **13**, 413 (2000).
[24] W.F. van Gunsteren, S.R. Billeter, A.A. Eising, P.H. Hünenberger, P. Krüger, A.E. Mark, W.R.P. Scott, I.G. Tironi. *Biomolecular Simulation: The GROMOS96 Manual and User Guide*, vdf Hochschulverlag, ETH Zürich, Switzerland (1996).
[25] W.R.P. Scott, P.H. Hunenberger, I.G. Tironi, A.E. Mark, S.R. Billeter, J. Fennen, A.E. Torda, T. Huber, P. Kruger, W.F. van Gunsteren. The GROMOS biomolecular simulation program package. *J. Phys. Chem. A*, **103**, 3596 (1999).
[26] W.F. van Gunsteren, X. Daura, A.E. Mark. GROMOS force field. In *Encyclopedia of Computational Chemistry*, P.v.R. Schleyer, N.L. Allinger, P.A. Kollman, T. Clark, H.F. Schaefer III, J. Gasteiger, P.R. Schreiner (Eds.), vol. 2, pp. 1211–1216, John Wiley & Sons, New York, NY (1998).
[27] P. Koehl, M. Levitt. *De Novo* protein design. In search of stability and specificity. *J. Mol. Biol.*, **293**, 1161 (1999).
[28] J. Aqvist, C. Medina, J. Samuelsson. New method for predicting binding affinity in computer-aided drug design. *Protein Eng.*, **7**, 385 (1994).
[29] R. Fraczkiewicz, W. Braun. Exact and efficient analytical calculation of the accessible surface areas and their gradients for macromolecules. *J. Comp. Chem.*, **19**, 319 (1998).
[30] D. Eisenberg, A.D. McLachlan. Solvation energy in protein folding and binding. *Nature*, **319**, 199 (1986).
[31] T.J. Richmond. Solvent accessible surface area and excluded volume in proteins. Analytical equations for overlapping spheres and implications for the hydrophobic effect. *J. Mol. Biol.*, **178**, 63 (1984).
[32] T.K. Harris, G.J. Turner. Structural basis of perturbed pK_a values of catalytic groups in enzyme active sites. *IUBMB Life*, **53**, 85 and references therein (2002).
[33] H. Li, A.D. Robertson, J.H. Jensen. Very fast empirical prediction and rationalization of protein pK_a values. *Proteins Struct. Funct. Bioinf.*, **61**, 704 (2005).